Internal Loop/Bulge and Hairpin Loop of the Iron-Responsive Element of Ferritin mRNA Contribute to Maximal Iron Regulatory Protein 2 Binding and Translational Regulation in the Iso-iron-responsive Element/Iso-iron Regulatory Protein Family

Yaohuang Ke,[‡] Hanna Sierzputowska-Gracz,[§] Zofia Gdaniec,[||] and Elizabeth C. Theil*,[‡]

CHORI (Children's Hospital Oakland Research Institute), Oakland, California 94609-1673, Department of Biochemistry and Chemistry, North Carolina State University, Raleigh, North Carolina 27696-7622, and Institute of Bioorganic Chemistry, Polish Academy of Sciences, Poznan, Poland

Received October 25, 1999; Revised Manuscript Received February 16, 2000

ABSTRACT: Iron-responsive elements (IREs), a natural group of mRNA-specific sequences, bind iron regulatory proteins (IRPs) differentially and fold into hairpins [with a hexaloop (HL) CAGUGX] with helical distortions: an internal loop/bulge (IL/B) (UGC/C) or C-bulge. C-bulge iso-IREs bind IRP2 more poorly, as oligomers ($n = 28-30$), and have a weaker signal response in vivo. Two trans-loop GC base pairs occur in the ferritin IRE (IL/B and HL) but only one in C-bulge iso-IREs (HL); metal ions and protons perturb the IL/B [Gdaniec et al. (1998) *Biochemistry 37,* 1505−1512]. IRE function (translation) and physical properties (T_m and accessibility to nucleases) are now compared for IL/B and C-bulge IREs and for HL mutants. Conversion of the IL/B into a C-bulge by a single deletion in the IL/B or by substituting the HL CG base pair with UA both derepressed ferritin synthesis 4-fold in rabbit reticulocyte lysates (IRP1 + IRP2), confirming differences in IRP2 binding observed for the oligomers. Since the engineered C-bulge IRE was more helical near the IL/B [$Cu(phen)_2$ resistant] and more stable (T_m increased) and the HL mutant was less helical near the IL/B (ribonuclease T1 sensitive) and less stable (T_m decreased), both CG trans-loop base pairs contribute to maximum IRP2 binding and translational regulation. The ^{1}H NMR spectrum of the Mg−IRE complex revealed, in contrast to the localized IL/B effects of Co(III) hexaammine observed previously, perturbation of the IL/B plus HL and interloop helix. The lower stability and greater helix distortion in the ferritin IL/B-IRE compared to the C-bulge iso-IREs create a combinatorial set of RNA/protein interactions that control protein synthesis rates with a range of signal sensitivities.

Awareness of mRNA regulation as a mechanism for controlling gene expression is increasing. The iso-IRE (iron responsive element)[1] family of mRNA regulatory elements recognized by the cognate proteins, iron regulatory proteins (IRPs), is one of the most extensively characterized mRNA regulatory targets. However, knowledge about mRNA regulation is in its infancy compared to understanding of DNA regulation such as hormone response elements recognized by hormone nuclear receptors (*1*). The ancient nature of the proteins encoded in IRE-containing, animal mRNAs (e.g., aconitase, ferritin), the homology of the IRPs to aconitases, and the recent detection of functional IREs and IRPs in bacteria (*2*) as well as animals suggest that the IRE/IRP interaction is also ancient, possibly representing regulation in an RNA world.

The common structural features of iso-IREs are a hairpin hexaloop (CAGUGX) with a trans-loop GC base pair and a helical stem (*3*−*5*). The GC base pair in the hexaloop has a large effect on the stabilization of the overall IRE structure (*3, 6*). A disordered C residue occurs in all IREs (*4, 5*). In many iso-IREs, the disordered C is a bulge in the helix of the IRE stem (*4*). In another type of iso-IRE, the disordered C residue is part of a set of four conserved residues [UGC-(16 nucleotides)-C] that form an internal loop/bulge (IL/B) with a trans-loop GC base pair (*5*). IRE sequences are mRNA-specific. IRE sequence differences in a single organism range from 36% to 85%, but for a particular mRNA, the IRE has high sequence conservation among animals, especially among vertebrates (>95%) (*7*).

Common structural features of iso-IRPs include protein kinase sites (*8, 9*) and sequence homology to aconitases (*10*), although no three-dimensional IRP structures are determined at this time. IRP1 binds Fe and sulfur with the acquisition of aconitase activity as cytosolic aconitase (*10*).

IRE-containing mRNAs have quantitatively different responses in vivo to an environmental signal such as iron (*11, 12*), allowing a range of response sensitivities to the same signal. Recently, in vitro studies of the IRE/IRP interaction, using short RNA sequences (28−30 nucleotides) from several different IRE-containing mRNAs and both recombinant and natural IRP1 and IRP2, showed different

[†] Partial support for this work came from NIH R01-DK-20251 and the CHORI Foundation.

* Corresponding author: CHORI (Children's Hospital Oakland Research Institute), 5700 Martin Luther King, Jr. Way, Oakland, CA 94609-1673. Tel (510) 450-7670; Fax (510) 597-7131; E-mail etheil@chori.org.

[‡] CHORI.

[§] NC State University.

[||] Polish Academy of Sciences.

[1] Abbreviations: IRE, iron-responsive element; IRP, iron regulatory protein; IL/B, internal loop/bulge; HL, iron-responsive element hairpin hexaloop (Hairpin Loop); RRL, rabbit reticulocyte lysate; TfR, transferrin receptor; WGE, wheat germ extract; WT, wild type.

10.1021/bi9924765 CCC: $19.00
Published on Web 04/26/2000

IRP2 binding among iso-IREs: the RNA/protein complexes and unbound RNA were separated by electrophoresis in native, sieving gels (*13*). The iso-IRE/IRP binding differences coincided with the range of different responses to iron in vivo (*11*−*13*). The differences in IRP2 binding to iso-IREs also correlated with differences between the IL/B and C-bulge and were abrogated by deletion of a conserved U residue from the internal loop/bulge to create a C-bulge (*13*).

To begin to connect the data on IRP binding for the short RNA sequence in vitro with the observed range of iron responsiveness in vivo, we now show that IRE-dependent regulation of protein synthesis in vitro reproduced the differences previously observed for iso-IRE binding to IRP1 and IRP2. In addition, decreases in translational repression and IRP2 binding were associated with either more or less distortion in the helix and more or less stability of the IRE structure, on the basis of $Cu(phen)_2$ or T1 probing and T_m measurements. Finally, NMR spectroscopy again emphasized the local sensitivity of the IL/B to metal ions observed previously (*5*) but also, since the hexaloop and interloop helix residues were perturbed, revealed the more global effects of Mg.

MATERIALS AND METHODS

Mutagenesis. IRE mutants in full-length transcripts, used to study IRE function in regulation of protein synthesis, were generated on the pBFH-1DV plasmid, which had been constructed by insertion of wild-type bullfrog H-subunit cDNA into pTZ19U vector (*14, 15*), by double-stranded, site-directed mutagenesis. The mutagenesis was done with a Chameleon double-stranded, site-directed mutagenesis kit (Stratagene) and followed the protocol provided by the manufacturer. The selection primer (5′-CTG TGA CTG GTG ACG CGT CAA CCA AGT C-3′) was designed to change the restriction endonuclease *Sca*I recognition site to the *Mlu*I site for enrichment and selection of IRE mutants. There is only one *Sca*I site in the vector of pBFH-1DV plasmid. The mutagenic primers were designed to produce IRE mutants. The sequences used are 5′-CAC TGT AGC AGA ACT CTA CTA AGA G-3′ (ΔU6 mutant), 5′-GGG TTC CGT TCA AAT ACT ATT GAA GCA AGA ACT CTA C-3′ (C14U/G18A mutant), and GGG TTC CGT TCA AAC ACT ATT GAA GCA AGA ACT CTA C (G18A mutant). The IRE mutants were confirmed by DNA sequencing with a T7 Sequenase version 2.0 DNA sequencing Kit (U.S. Biochemical Corp.).

RNA Preparation. Capped full-length RNA transcripts were transcribed from pBFH-1DV and the derived mutant (pBFH-ΔU6, pBFH-C14U/G18A, and pBFH-G18A) generated by mutagenesis. The plasmids were digested with *Sal*I restriction endonuclease, 24 nucleotides downstream from the DNA sequence encoding the ferritin mRNA poly(A)+ tail. The linearized plasmids were purified by extraction with phenol, phenol/chloroform, and chloroform, precipitated with ammonium acetate and ethanol, and then used as templates for transcription. Transcription reactions were performed as described previously (*14*−*16*) except for the omission of radioactive nucleotide in the reactions. The transcription products were purified through RNeasy columns (Qiagen) and eluted in H_2O. The purified transcript was quantitated by reading the absorbance at 260 nm at various dilutions and stored at −80 °C. Homogeneity of the transcripts was analyzed on 1 M urea/1.5% agarose gels.

RNAs (29−30-mer) used for thermal denaturation and enzymatic and chemical structure probing were transcribed from chemically synthesized DNA templates with T7 RNA polymerase (*6, 17*), followed by gel purification and ethanol precipitation, and then resuspended in H_2O and stored at −80 °C until use. RNA labeling was performed as described previously (*18, 19*), with purification through NENsorb columns (DuPont). The RNAs used for thermal denaturation were further purified by dialysis against H_2O.

For NMR analysis, the ferritin IRE 30-mer was synthesized and gel-purified by the CyberSyn Company in Lenni, PA. Samples for the analysis were prepared by dissolving approximately 1.1 mg of the purified RNA in 0.2 mL of 90% H_2O/10% D_2O phosphate buffer (10 mM sodium phosphate, pH 6.8, and 0.1 mM EDTA) to give ∼0.5 mM RNA. The samples were heated at 80 °C for 5 min and cooled slowly prior to each experiment. Mg^{2+} was added after annealing. Aliquots of the stock solution of 0.3 mM $MgCl_2$ were individually added to the RNA sample to produce different ratios of the divalent ions to RNA. At the strand concentration used ≫90% of the RNA was monomeric, on the basis of melting profiles and diffusion NMR analysis.

Protein Synthesis in Vitro. Nuclease-treated rabbit reticulocyte lysates (RRL) and wheat germ extracts (WGE) from Promega were used for protein synthesis as previously described (*14, 15, 20, 21*). Ferritin synthesis with [^{35}S]-methionine labeling in RRL was carried out at 30 °C for 17 min and in WGE at 25 °C for 40 min. The final concentration of full-length transcripts directing ferritin synthesis is 1.5 nM in RRL and 3.0 nM in WGE. Ferritin synthesis rates were linearly dependent on the incubation time and RNA concentration on the basis of preliminary experiments with different incubation times and RNA concentrations. After termination of the labeling translation reactions with an equal volume of 10 mM cold methionine, the labeled, synthesized ferritin was resolved by SDS−polyacrylamide gel electrophoresis and analyzed with a PhosphorImager and ImageQuant software (Molecular Dynamics).

Enzymatic and Chemical Structure Probing. Cleavage of RNA with T1 and $Cu(phen)_2$ complexes followed the previous description (*18, 19*) with modifications. 5′-^{32}P-Labeled RNAs were melted at 85 °C for 5 min and then slowly annealed in a metal block at room temperature before incubation with RNase T1 or $Cu(phen)_2$ under native conditions. Cleavage by the transition metal complex was initiated with 3-mercaptopropionic acid at 25 °C and terminated with 2,9-dimethyl-1,10-phenanthroline after 5 min. Digestion with T1 under denaturing conditions and alkaline hydrolysis of RNA for gel calibration have been previously described (*18*). The cleavage products were resolved by electrophoresis in a denaturing gel (*18*) and analyzed with a PhosphorImager and ImageQuant software (Molecular Dynamics).

Thermal Denaturation. Wild-type or mutant IRE (∼1.5 μM in 10 mM phosphate buffer, pH 6.8, with or without 100 mM NaCl) were heated and annealed, as described under Enzymatic and Chemical Structure Probing, prior to thermal denaturation analysis. RNA thermal denaturation over the range of 5−95 °C used 1 cm path length, reduced-volume,

quartz cells (800 μL). The thermal denaturation profiles, absorbance at 260 nm as a function of temperature, were acquired on a Cary 100 spectrophotometer system with accessories for thermal melting. The rate of temperature increase was 1 °C/min. Melting temperature (T_m) and free energy (ΔG_{37}) were determined with hypochromicity methods (Cary Win Bio package application software).

NMR Spectroscopy. NMR spectra were obtained on a Bruker AVAVCE 500 MHz spectrometer (1990) with an Oxford narrow-bore magnet (1989), SGI INDY Host Workstation, XWINNMR software. Spectra in 10%/90% D_2O/H_2O were acquired with a triple-gradient probe and WATERGATE pulse sequence for water suppression (*22*). Spectra acquired at 4 or 12 °C showed no detectable difference. Spectra were processed with XWINNMR software and Felix software (MSI), using exponential weighting function or shifted sine-bell function to resolve overlapped imino protons.

RESULTS

Effects of Mutations in the Internal Loop/Bulge or Hairpin Loop on Translation Repression. To determine if the internal loop/bulge (IL/B) and C-bulge IREs' effect on translational regulation of protein synthesis was the same as on IRP2 binding in vitro (*13*), ferritin synthesis directed by 5′-capped, 3′-polyadenylated, full-length ferritin mRNA was compared for RNA with wild type (IL/B) IRE or ΔU6 (C-bulge) IRE sequences (Figure 1). Previous studies had shown that the engineered C-bulge ferritin IRE, ΔU6, displays the same type of IRP2 binding as natural C-bulge IREs (erythroid aminolevulinate synthase, mitochondrial aconitase, and transferrin receptor IREs) and contrasts with the wild-type (WT) ferritin IRE containing an IL/B in protein binding assays (*13*). The ferritin ΔU6 IRE sequence thus is a useful model for comparisons of C−bulge and IL/B IREs, since other variations in sequence among natural IREs with a C-bulge will not be a factor. Included for comparison are data with full-length transcripts of ferritin mRNA containing the IRE hairpin loop (HL) mutations G18A or C14U/G18A (Figure 1A) that had previously been studied with a human growth hormone (hGH) reporter in transfected cells (*23*). Ferritin synthesis directed by the G18A-IRE ferritin full-length transcript, which had also previously been shown to be completely derepressed in rabbit reticulocyte lysates (RRL) (*24*), made a useful control for IRE-independent experimental variations.

Translation conditions were selected so that the rates of ferritin synthesis were linearly dependent on incubation time and mRNA concentration. RRL was selected because it had previously been shown to regulate ferritin mRNA with trans factors (*14*, *21*, *25*−*27*), now known to be IRP1 and IRP2 (*13*). In addition, ferritin synthesis in wheat germ extracts was measured to assess possible general effects of the mutations on protein synthesis, since wheat germ extracts have no ferritin mRNA-specific regulation (no IRPs) (*21*, *25*, *28*).

The results showed that all mutations in the IRE region studied increased ferritin synthesis in RRL, suggesting IRE-dependent derepression of translation (Figure 1B). However, deletion of U6 in the IL/B region or C14U/G18A double mutations in the HL increased ferritin synthesis by 4-fold while G18/A IRE mutation in the HL caused a 13-fold increase in translation. In wheat germ extract, which has no IRE recognition proteins (*25*, *28*), all the transcripts tested were identical in directing ferritin synthesis (Figure 1C), showing that the differences in ferritin synthesis in RRL were dependent on IRP-regulated protein synthesis.

Table 1: IRE-Dependent Translation Repression and IRP Binding to the IRE

ferritin mRNA	repression in RRL[a]	binding to the IRE in ferritin mRNA	
		IRP1[b]	IRP2[b]
WT	94 ± 3	100	100
ΔU6	66 ± 3	87 ± 5	<5
C14U/G18A	64 ± 6	89 ± 4	<5
G18A	0[c]	<1	<1

[a] Ferritin synthesis in RRL was analyzed by electrophoresis (Figure 1B) and quantitated by use of a PhosphorImager and ImageQuant software. The data are average of three experiments with two independent preparations of RNA in vitro transcripts. Repression = (1 − ferritin synthesis/G18A transcript-directed ferritin synthesis) × 100. [b] Data from ref *13*. [c] Repression for G18A ferritin mRNA was set to be zero, as neither IRP1 nor IRP2 binds the IRE in the mRNA, and was used to calculate repression for other tested ferritin mRNAs.

To facilitate quantitative comparisons of the effects of IRE structure on ferritin mRNA function, the data were normalized to those obtained with mRNA containing the G18A IRE, since neither IRP1 nor IRP2 is bound by the G18A IRE (*13*, *29*−*31*) and ferritin synthesis is fully derepressed in RRL (*24*). The ΔU6 transcript was only repressed by 66% ± 3%, whereas the repression for the WT transcript was 94% ± 3% (Table 1). Repression of the C14U/G18A IRE transcript in RRL (64% ± 6%) was comparable to the ΔU6 IRE transcript (Table 1) and confirms the results obtained with the same mutation and a hGH reporter transfected into cultured cells (*23*).

Effects of Internal Loop/Bulge and Hairpin Loop Mutations on Thermal Stability. The helix distortion, C-bulge, or internal loop/bulge (IL/B) in the iso-IREs influences both IRP2 recognition (*13*) and translation repression (Figure 1 and Table 1). The main structural difference between these two types of IREs is the number of nucleotides involved in the distortion at the midpoint of the helix (Figure 2). To explore the structural variation in the helix distortion and to examine the relationship of the helix distortion to IRE function, the thermal stability was analyzed for a series of IREs.

Conversion of the IL/B to a C-bulge by deletion of U6 increased the T_m and thermal stability (Table 2) as predicted from the change in secondary structures (Figure 2). Substitution of the hairpin loop (HL) CG base pair by UA (Figure 3) decreased T_m and thermal stability but had less effect than disruption of the base pair with a single mutation in the HL (G18A IRE) (Table 2), emphasizing the importance of the base pair in the HL to IRE stability. All these mutants, whether destabilizing or stabilizing IRE structures, decreased IRP2 binding (*13*) and translational regulation (Figure 1), suggesting that the RNA structure of the ferritin IRE is precisely balanced in an energy state associated with optimum protein recognition.

Effects of Internal Loop/Bulge and Hairpin Loop Mutations on Access to Nucleases: Cu(phen)$_2$ and RNase T1. $Cu(phen)_2$, a small reagent, was used to probe the structure of iso-IREs that displayed different binding of IRP2.

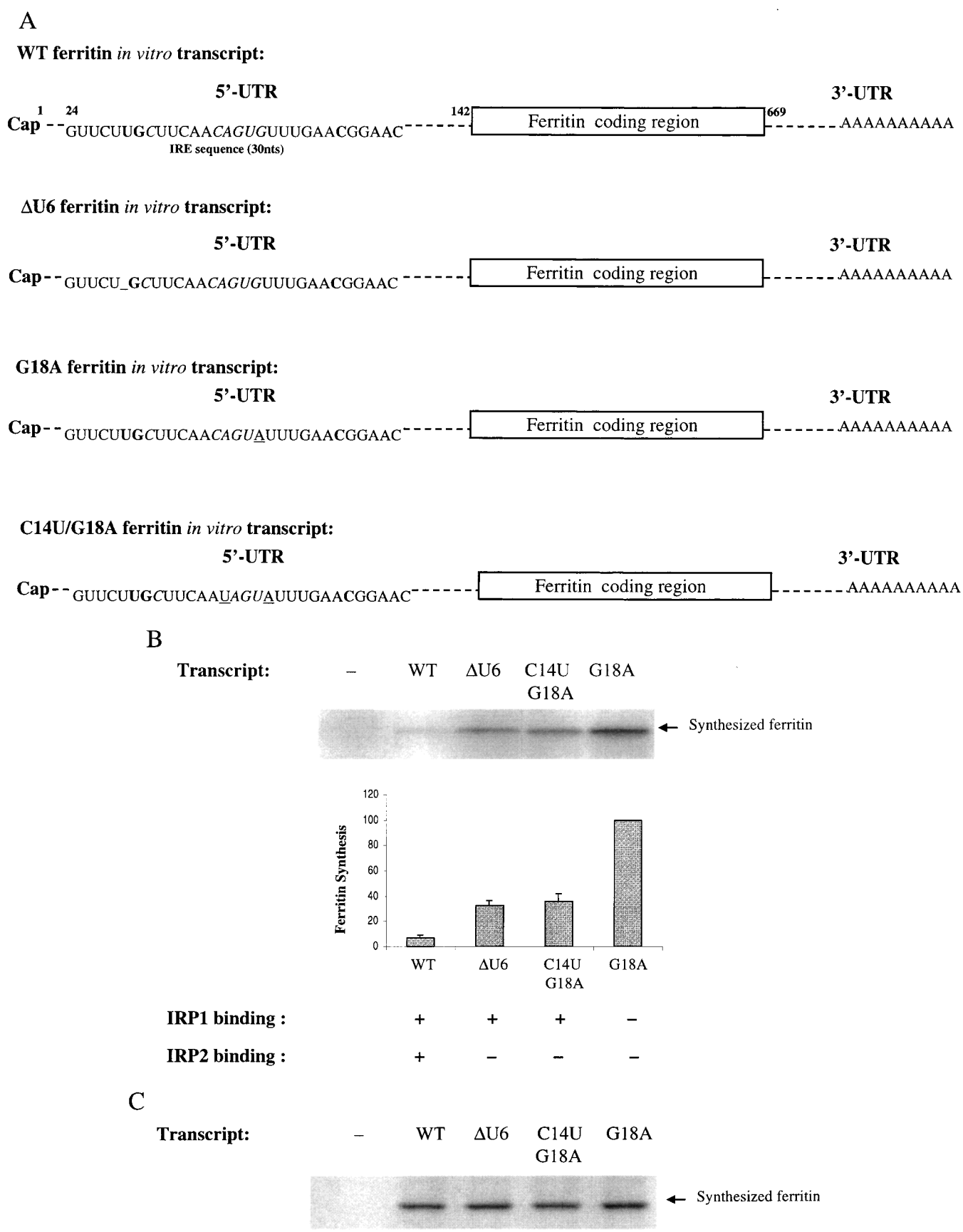

FIGURE 1: Effects of the IRE helix distortion (IL/B or C-bulge) on ferritin synthesis. Capped, polyadenylated full-length transcripts with the IL/B, C-bulge, and HL mutant IRE, schematically presented in panel A, were translated in rabbit reticulocyte lysates (B) or in wheat germ extracts (C) with [^{35}S]methionine. Ferritin synthesis was analyzed by electrophoresis in an SDS−polyacrylamide gel and with a PhosphorImager (Molecular Dynamics). The gel picture shown (B, C) is representative of three experiments with two independent preparations of the RNA transcripts. The wild-type and mutant ferritin IRE sequences are shown in panel A. Italic type indicates conserved residues in iso-IREs; boldface type indicates ferritin IRE-specific residues; underlined residues are mutant residues/sites in the 5′ untranslated region.

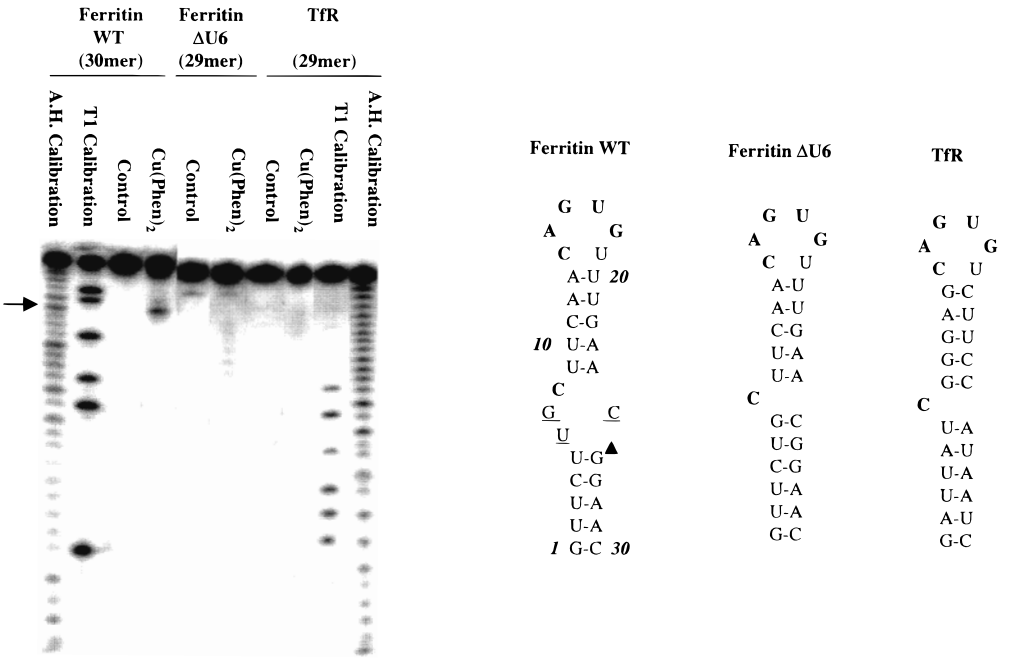

FIGURE 2: Effects of the IRE helix distortion (IL/B or C-bulge) on reactivity with $Cu(phen)_2$ complexes. 5′-^{32}P Labeled wild-type and mutant IREs (sequences and secondary structures on the right of the figure) were heated and slowly annealed as described under Materials and Methods. The annealed RNAs were incubated with or without $Cu(phen)_2$, followed by initiation of the cleavage with 3-mercaptopropionic acid at 25 °C and termination of the cleavage with 2,9-dimethyl-1,10-phenanthroline after 5 min. The cleavage products were resolved by electrophoresis and analyzed with a PhosphorImager and ImageQuant software (Molecular Dynamics). The experiment was repeated for 3−4 times with two independently prepared RNAs for each IRE. WT, wild type; ΔU6, ferritin IRE with a single U deletion in the IL/B; TfR, transferrin receptor; A.H. calibration, alkaline hydrolysis of WT ferritin or TfR IRE; T1 calibration, RNase T1 cleavage of denatured WT or TfR IRE; control, without $Cu(phen)_2$; $Cu(phen)_2$, cleavage with $Cu(phen)_2$. The arrow shows the site at which $Cu(phen)_2$ cleavage was changed by engineered or natural mutations. The cleavage sites are also shown in the secondary structures (▲); a significant cleavage site has >10× the intensity on average compared to insignificant cleavage sites. Note that the $Cu(phen)_2$ reactivity was not significantly changed in the IRE with the C14U/G18A hairpin loop mutation (for clarity these data are not shown).

Table 2: Effects of Loop Mutations on Structures in Other Loops in the Ferritin IRE, Thermal Stability, and IRP2 Binding

IRE sequence[a]	IRP2 binding[b]	Reactivity[c]			T_m[d] (°C)	ΔG_{37}[d] (kcal/mol)
		IL/B(G26/G27)		HL(G18)		
		$Cu(phen)_2$	RNase T1	RNaseT1		
WT	+	+	−	−	47.0 ± 0.7	−2.2 ± 0.2
HL C14U/G18A	−	+	+	na[e]	44.4 ± 1.0	−1.6 ± 0.1
HL G18A	−	+	+	na[e]	42.5 ± 0.9	−1.1 ± 0.1
IL/B ΔU6	−	−	−	−	52.3 ± 0.8	−3.8 ± 0.1
IL/B ΔU6, ΔG7[f]	nd[g]	−	−	+	nd[g]	nd[g]

[a] HL; hairpin loop (CAGUGX; residues 14−18); IL/B; internal loop/bulge (UGC/C; residues 6, 7, 8/25). Note that the chemical shifts of imino proton resonances of loop residues U6, G7, G26 and G27, and G18 are all affected by Mg. RNase T1 reactivity toward the G residues in the HL is changed by IL/B mutation and reactivity toward the IL/B by HL mutation, emphasizing the structural interdependence of different parts of the ferritin IRE. Both types of changes eliminate IRP2 binding (*13*). [b] Data from (*13*). [c] See Materials and Methods and Figures 2 and 3. [d] Wild-type or mutant IRE (∼1.5 μM; for sequences and secondary structures, see Figures 2 and 3) in 1 mL of 10 mM phosphate buffer, pH 6.8, was thermally denatured between 5 and 95 °C. The denaturation profile, absorbance at 260 nm as a function of temperature, was acquired on a Cary 100 spectrophotometer system. T_m and ΔG_{37} were determined from the profiles with hypochromicity methods (Cary Win Bio package application software). The data are the average of 3−4 experiments with two independently prepared RNA samples for each IRE; the error is presented as the standard deviation. Thermal denaturation of the RNAs in the phosphate buffer with 100 mM NaCl was also performed. For one experiment, the T_m (ΔG_{37}) for WT, ΔU6, C14U/G18A, and G18A IREs are 55.0 °C (−4.6 kcal/mol), 60.8 °C (−6.1 kcal/mol), 52.5 °C (−3.8 kcal/mol), and 50.5 °C (−2.6 kcal/Mol), respectively. [e] Not applicable, because the potential substrate, G, is replaced by A. [f] Data taken from ref *24*. [g] Not determined.

Reactivity of a ferritin IRE with a single deletion in the internal loop/bulge (IL/B) (ferritin ΔU6 IRE) and the natural C-bulge IRE (transferrin receptor IRE) was compared to that of the wild-type (WT) ferritin IRE. The $Cu(phen)_2$ complex is a small (∼13 Å and 460 Da), structure-specific, sequence-independent probe that cleaves distortions in RNA helices (*32*−*34*) including the ferritin IRE (*18, 19, 35*).

The results showed that $Cu(phen)_2$ cleaved the IRE 30-mer at G26 adjacent to the IL/B (Figure 2), as previously observed with natural mRNA or full-length ferritin in vitro transcript (*18, 19, 35*). In contrast, no $Cu(phen)_2$ cleavage was observed for either the engineered (ΔU6) or the natural (TfR) C-bulge IRE (Figure 2). Cleavage of the IRE was unaffected by the C14U/G18A Hairpin Loop (HL) mutation (data not shown in Figure 2 for clarity).

Thermal denaturation studies of WT and mutant ferritin IREs (Table 2) indicate that the GC base pair in the HL increases the overall stability by 50%. Given the diminished effect of mutating the G of the GC base pair in the HL on the stability of an IRE 16-mer (15%) (*3*), an effect of the

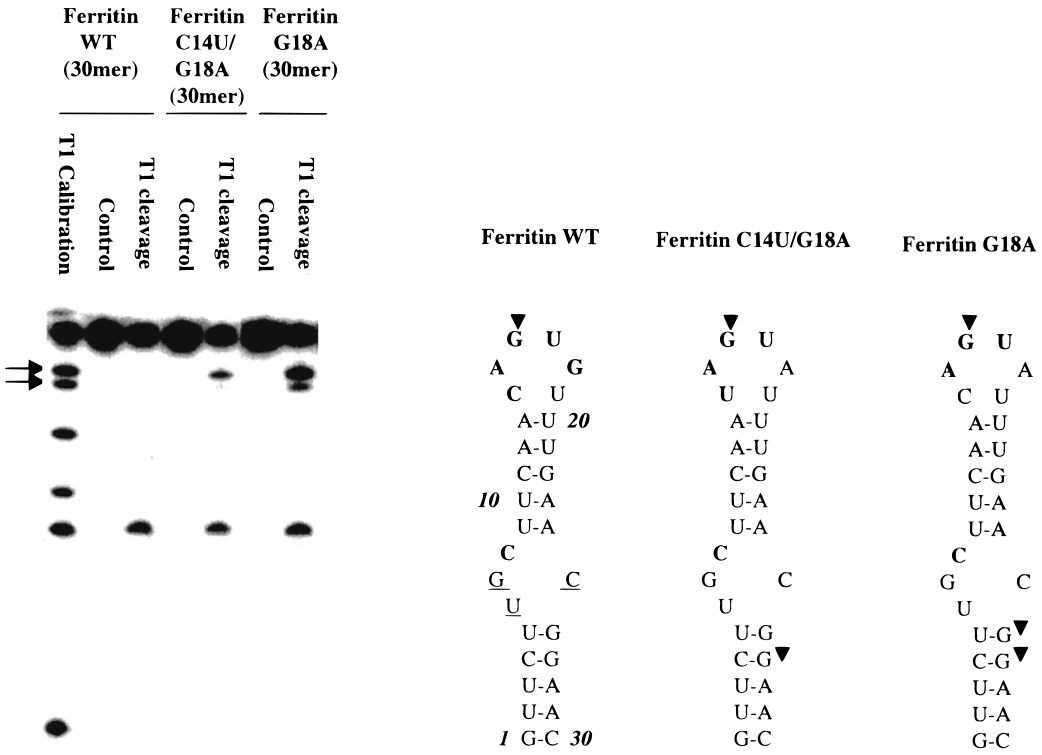

FIGURE 3: Effects of the hairpin loop mutations on RNase T1 cleavage at the IRE helix distortion. 5′-^{32}P-labeled wild-type and mutant IREs (sequences and secondary structures on the right of the figure) were heated and slowly annealed as described under Materials and Methods. RNase T1 cleavage of the annealed RNAs was accomplished by incubation of the RNAs with RNase T1 at 25 °C for 7 min. The cleavage products were resolved by electrophoresis and analyzed with a PhosphorImager and ImageQuant software (Molecular Dynamics). The experiment was repeated 3−4 times with two independently prepared RNAs for each IRE. WT, wild type; T1 calibration, RNase T1 cleavage of denatured WT IRE; control, incubation without RNase T1; T1 cleavage, incubation with RNase T1. Arrow shows the site in the IL/B at which RNase T1 cleavage was changed by mutation in the hairpin loop. The cleavage sites, shown in the secondary structures (▼), have >10× the intensity on average compared to insignificant cleavage sites. Note that the RNase T1 reactivity was unchanged in the ΔU6 IRE (for clarity these data are not shown).

HL mutation on the IL/B or helix structure is suggested. However, the small probe Cu(phen)$_2$ (∼13 Å and 460 Da) did not detect structural changes in the HL mutant IRE.

RNase T1 is a larger probe (∼30 Å and11 000 Da) in contrast to the Cu(phen)$_2$ complex (*32*). Neither G26 nor G27 adjacent to the IL/B is cleaved by RNase T1 in the ferritin WT IRE (Figure 3) at room temperature (*18, 19, 36*), although G26 and G27 are cleaved by the smaller Cu(phen)$_2$ probe in the IRE 30-mer (Figure 2) and ferritin mRNA (*18, 19*). [Note that at high temperatures (45−50 °C), the G residues (G7 and G18) in the GC trans-loop base pairs are cleaved by RNase T1, revealing differential thermal stability compared to other regions of the helix (*18, 19, 36*).] The data in Figure 3 show that mutations in the HL at residues 14 and 18, which decreased IRP2 binding (*5*), translation repression (Figure 1), and T_m (Table 2), also changed structure around the IL/B, even though the sites of the mutations are more than 22 Å away from the IL/B (*5*). The mutations increased the sensitivity of G26 and G27 to RNase T1.

Effect of Mg^{2+} on the ^1H NMR spectrum of the Iron-Responsive Element. Previous NMR data and molecular modeling of Co(III) hexaammine binding to ferritin IRE indicated that the internal loop/bulge (IL/B) is a Co(III) hexaammine binding site (*5*). In addition, the IL/B is very sensitive to mutation and pH (Figures 2 and 3) (*5, 24*). Since Mg^{2+} is a physiological regulator of RNA structure and since both Co(III) hexaammine and Mg hexahydrate can bind at similar sites in other RNAs (*37, 38*), the possibility that Mg binds in the IL/B was explored with one-dimensional NMR spectroscopy.

The ^{1}H NMR spectrum of the ferritin IRE with or without Mg^{2+} is shown in Figure 4A. Quantitation of Mg-induced change of chemical shifts of IRE imino proton resonances is shown in Figure 4B. Mg^{2+} produced a significant change of the chemical shifts of imino proton resonance for G26, G27, U5, U6, and G7 (Figure 4), which are all located in the IL/B, as did Co(III) hexaammine. However, Mg also induced significant chemical shifts for residues U10 and U21, in the helix between the IL/B and the hairpin loop (HL), and for G18, part of the base pair across the HL (Figure 4). The same sites for which Mg shifted the proton resonances were affected by Mg when Cu(phen)$_2$ cleavage was used to probe the structure of the IRE in natural poly(A)+ ferritin mRNA (*18, 35*). The results could reflect charge effects of Mg bound to the RNA complex or could indicate a structural change in the RNA.

DISCUSSION

A range of responses to cytoplasmic signals, such as iron, is possible among the mRNAs that contain IREs (*11, 12, 39*) despite the similarity of the iso-IRE secondary structure. All iso-IREs have the hairpin hexaloop (HL) with the conserved sequence CAGUGX and the helix distortion with a disordered C residue (*4, 5, 7, 40−42*). The range of physiological responses to iron among the mRNA with iso-IREs coincides with differences in binding of IRP2 (*13*). Two

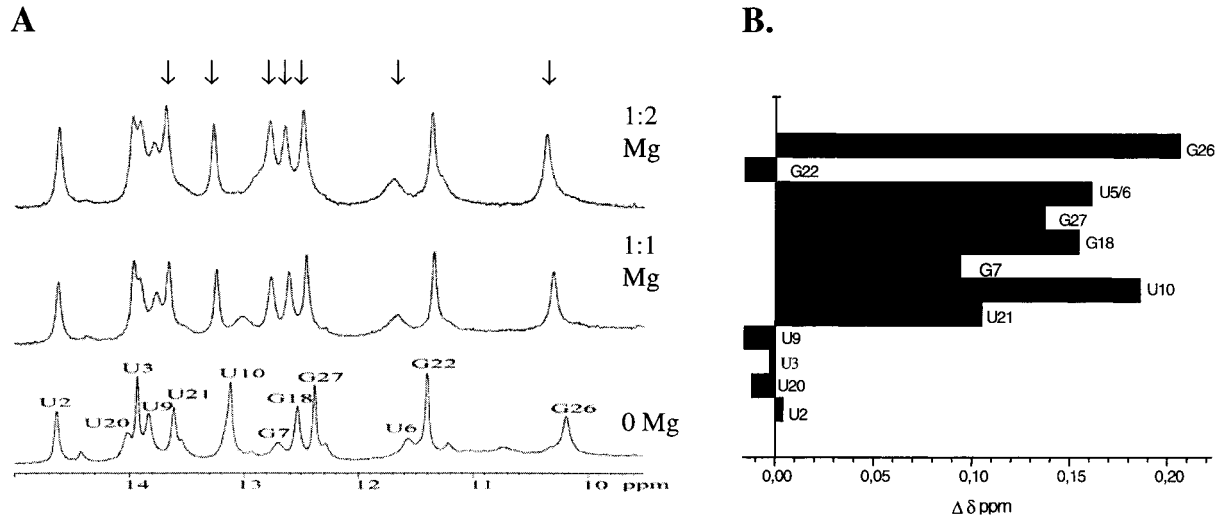

FIGURE 4: Effects of Mg^{2+} on chemical shifts of IRE imino resonances. The ^1H NMR spectrum of the ferritin IRE (0.5 mM RNA) was collected at 12 °C in 10 mM sodium phosphate and 0.1 mM EDTA, pH 6.8, with or without Mg $^{2+}$. (A) ^1H NMR spectra. Arrows show chemical shifts of imino proton resonances significantly upshifted by Mg (see panel B). The chemical shifts are for the residues in the IL/B, the HL, or the stem between them; no significant change of the chemical shifts for the residues in the lower stem was observed. (B) Quantitative comparison of Mg-induced shift of chemical shifts of imino proton resonances.

types of helix distortions known in the iso-IREs are a C-bulge (*4*) and an internal loop/bulge (IL/B) that contains the C residue. In the ferritin IRE, the IL/B forms a pocket that appears to bind Co(III) hexaammine and has a pH-dependent conformation (*5*). Coincidentally, the ferritin mRNA, which contains the IL/B iso-IRE, has the greatest range of iron regulation of any of the IRE-containing mRNAs both in vitro and in vivo (*11, 12, 43*−*47*). Even in an IL/B mRNA constructed from a ferritin IRE plus a human growth hormone (hGH) sequence, the ferritin IRE is more efficiently regulated than the transferrin receptor IRE (C-bulge) in the comparable hGH construct (*48*). In addition to the IL/B or C-bulge, the stem sequences among IREs in different mRNAs can diverge as much as 65% (*7*). Recently, differences in IRE/IRP interaction in vitro (*13*) were shown to coincide with the wide range of iron responses by IRE-containing mRNAs previously observed in vivo (*11*).

A connection between the different iron responses of IRE-containing mRNAs in rat liver (*11*) and the differential binding of IRP-1 and IRP-2 to short iso-IREs (29 and 30 nucleotides) in vitro (*13*) is shown by the correlation between translational repression in vitro of full-length, poly(A)+ mRNAs, IRE/IRP binding, the iron-induced rates of protein synthesis in vivo, and the presence of an IL/B or C-bulge in the IRE (Figure 1) (*11*−*13, 43*−*48*). IRP2 binding to the IRE is sensitive to the natural or engineered variation in the helix distortion (*13*) or to the engineered variation in the hairpin loop (*29*−*31*).

Chemical and enzymatic probing of IREs connects IRE structure with function measured as IRP2 binding and translation regulation (Table 2). Whether mutations were made in the HL or the IL/B, all mutations tested that displayed diminished IRP2 binding or translation repression also altered IL/B sensitivity to nuclease attack. For example, RNase T1 showed that the HL mutations made changes reflected in localized helix distortions near the IL/B 22 Å away (Figure 3 and Table 2), while the small probe $Cu(phen)_2$ detected localized effects of mutation in the IL/B itself (Figure 2 and Table 2). ^{31}P NMR spectra of wild-type (WT) and HL mutant (G18A) IREs from previous NMR analysis (*6*) also indicated global perturbations in the helix backbone. Effects of the IL/B mutation on the HL were less dramatic than the effect of HL mutations on the IL/B and could not be detected with RNase T1 for the single deletion (Table 2). However, in a double IL/B deletion mutant (ΔU6 +ΔG7), both RNase T1 (Table 2) and [Ru(tpy)(bpy)] (*24*) showed increased access to the HL. Clearly, the mutation in either loop region of the ferritin IRE influences the other loop and emphasizes interdependence of structural features throughout the ferritin IRE. [Preliminary data, (Ke and Theil, unpublished results) show that the thermal denaturation of the ferritin IRE is much more cooperative than that of any of the other IREs.]

Both IRE loops, the HL and IL/B, contribute to the specificity of IRP2 binding and translation repression (Figure 1 and Table 1), but the effects on the properties of the helix distortion around the conserved C residues differ. For example, disruption of the CG base pair or replacement of it with UA in the HL decreased the base stacking in the IRE (decreased T_m) (Table 2) and increased the helix distortion around the IL/B (increased sensitivity to RNase T1) (Figure 3). On the other hand, deletion of U6 in the IL/B increased base stacking in the IRE (increased T_m) (Table 2) and decreased the helix distortion at the IL/B [resistance to $Cu(phen)_2$ cleavage] (Figure 2). Thus, the CG trans-loop base pair in the HL appears to decrease distortions in the IRE, whereas the CG trans-loop base pair in the IL/B is associated with increased distortion in the helix near the conserved C residue. How the effects of Mg on IL/B, HL, and helix residues, detected by NMR spectroscopy (Figure 3) and $Cu(phen)_2$ cleavage (*18*), relate to IRE function has not yet been determined, but they may contribute to kinetics of protein binding. The negative impact of either destabilizing the IRE (HL mutations) or stabilizing the IRE (IL/B mutations) on IRP2 binding and translation repression (Figure 1 and Table 2) indicates that the native ferritin IRE structure (HL + IL/B) has the optimum stability and site accessibility for IRP2 binding and translation regulation. Iso-IRE RNA isoform

variation, illustrated by the distinctive properties of the ferritin IRE, provides a natural set of mRNA-specific regulatory sequences. The combinatorial RNA/protein interactions possible with iso-IREs and iso-IRPs yield a range of mRNA responses to a single environmental signal.

REFERENCES

1. Darimont, B. D., Wagner, R. L., Apriletti, J. W., Stallcup, M. R., Kushner, P. J., Baxter, J. D., Fletterick, R. J., and Yamamoto, A. R. (1998) *Genes Dev. 12*, 3343−3356.
2. Alen, C., and Sonenshein, A. L. (1999) *Proc. Natl. Acad. Sci. U.S.A. 96*, 10412−10417.
3. Liang, L. G., and Hall, K. B. (1996) *Biochemistry 35*, 13586−13596.
4. Addess, K. J., Basilion, J. P., Klausner, R. D., Rouault, T. A., and Pardi, A. (1997) *J. Mol. Biol. 274*, 72−83.
5. Gdaniec, Z., Sierzputowska-Gracz, H., and Theil, E. C. (1998) *Biochemistry 37*, 1505−1512.
6. Sierzputowska-Gracz, H., McKenzie, R. A., and Theil, E. C. (1995) *Nucleic Acids Res. 23*, 145−152.
7. Theil, E. C. (1998) in *Metal Ions in Biological Systems. Iron Transport and Storage in Microorganisms, Plants, and Animals* (Sigel, A., and Sigel, H., Eds.) pp 403−434, Marcel Dekker, Inc., New York.
8. Eisenstein, R. L., Tuazon, P. T., Schalinske, K. L., Anderson, S. A., and Traugh, J. A. (1993) *J. Biol. Chem. 268*, 27363−27370.
9. Schalinske, K. L., and Eisenstein, R. S. (1996) *J. Biol. Chem. 271*, 7168−7175.
10. Beinert, H., Kennedy, M. C., and Stout, C. D. (1996) *Chem. Rev. 96*, 2335−2373.
11. Chen, O. S., Schalinske, K. L., and Eisenstein, R. S. (1997) *J. Nutr. 127*, 238−248.
12. Schalinske, K. L., Chen, O. S., and Eisenstein, R. S. (1998) *J. Biol. Chem. 273*, 3740−3746.
13. Ke, Y., Wu, J., Leibold, E. A., Walden, W. E., and Theil, E. C. (1998) *J. Biol. Chem. 273*, 23637−23640.
14. Dix, D. J., Lin, P.-N., Kimata, Y., and Theil, E. C. (1992) *Biochemistry 31*, 2818−2822.
15. Dix, D. J., Lin, P.-N., McKenzie, A. R., Walden, W. E., and Theil, E. C. (1993) *J. Mol. Biol. 231*, 230−240.
16. Fletcher, L., Corbin, S. D., Browning, K. S., and Ravel, J. M. (1990) *J. Biol. Chem. 265*, 19582−19587.
17. Milligan, J. F., and Uhlenbeck, O. C. (1989) *Methods Enzymol. 180*, 51−62.
18. Wang, Y.-H., Sczekan, S. R., and Theil, E. C. (1990) *Nucleic Acids Res. 18*, 4463−4468.
19. Harrell, C. M., McKenzie, A. R., Patino, M. M., Walden, W. E., and Theil, E. C. (1991) *Proc. Natl. Acad. Sci. U.S.A. 88*, 1−6.
20. Shull, G. E., and Theil, E. C. (1982) *J. Biol. Chem. 257*, 14187−14191.
21. Dickey, L. F., Wang, Y.-H., Shull, G. E., Wortman, I. A., III, and Theil, E. C. (1988) *J. Biol. Chem. 263*, 3071−3074.
22. Piotto, M., Saudek, V., and Sklenar, V. (1992) *J. Biomol. NMR 2*, 661−665.
23. Menotti, E., Henderson, B. R., and Kuhn, L. C. (1998) *J. Biol. Chem. 273*, 1821−1824.
24. Thorp, H. H., McKenzie, R. A., Lin, P.-N., Walden, W. E., and Theil, E. C. (1996) *Inorg. Chem. 35*, 2773−2779.
25. Walden, W. E., Daniels-McQueen, S., Brown, P. H., Gaffield, L., Russell, D. A., Bielser, D., Bailey, L. C., and Thach, R. E. (1988) *Proc. Natl. Acad. Sci. U.S.A. 85*, 9503−9507.
26. Leibold, E. A., and Munro, H. N. (1988) *Proc. Natl. Acad. Sci. U.S.A. 85*, 2171−2175.
27. Bhasker, C. R., Burgiel, G., Neupert, B., Emery-Goodman, A., Kuhn, L. C., and May, B. K. (1993) *J. Biol. Chem. 268*, 12699−12705.
28. Rothenberger, S., Mullner, E. W., and Kuhn, L. C. (1990) *Nucleic Acids Res. 18*, 1175−1179.
29. Henderson, B. R., Menotti, E., Bonnard, C., and Kuhn, L. C. (1994) *J. Biol. Chem. 269*, 17481−17489.
30. Henderson, B. R., Menotti, E., and Kuhn, L. C. (1996) *J. Biol. Chem. 271*, 4900−4908.
31. Butt, J., Kim, H.-Y., Basilion, J. P., Cohen, S., Iwai, K., Philpott, C. C., Altschul, S., Klausner, R. D., and Rouault, T. A. (1996) *Proc. Natl. Acad. Sci. U.S.A. 93*, 4345−4349.
32. Theil, E. C. (1994) *New J. Chem. 18*, 435−441.
33. Murakawa, G. J., Chen, C. B., Kuwabara, M. D., Nierlich, D. P., and Sigman, D. S. (1989) *Nucleic Acid Res. 17*, 5362−5375.
34. Sigman, D. S. (1990) *Biochemistry 29*, 9097−9105.
35. Wang, Y.-H., Sczekan, S. R., McKenzie, R. A. and Theil, E. C. (1991) *Biol. Met. 4*, 56−61.
36. Bettany, A. J. E., Eisenstein, R. S., and Munro, H. M. (1992) *J. Biol. Chem. 267*, 16531−16537.
37. Cate, J. H., and Doudna, J. A. (1996) *Structure 4*, 1221−1229.
38. Kieft, J. J., and. Tinoco, I. (1997) *Structure 5*, 713−721.
39. Eisenstein, R. S., and Blemings, K. P. (1998) *J. Nutr. 128*, 2295−8.
40. Theil, E. C. (1994) *Biochem. J. 304*, 1−11.
41. Rouault, T. A., and Klausner, R. D. (1996) *J. Biol. Inorg. Chem. 1*, 494−499.
42. Hentze, M. W., and Kuhn, L. C. (1996) *Proc. Natl. Acad. Sci. U.S.A. 93*, 8175−8182.
43. Schaefer, F. V., and Theil, E. C. (1981) *J. Biol. Chem. 256*, 1711−1715.
44. Shull, G. E., and Theil, E. C. (1983) *J. Biol. Chem. 258*, 7921−7923.
45. Dandekar, T., Stripecke, R., Gray, N. K., Goossen, B., Constable, A., Johansson, H. E., and Hentze, M. W. (1991) *EMBO J. 10*, 1903−1909.
46. Melefors, O., Goossen, B., Johansson, H. E., Stripecke, R., Gray, N. K., and Hentze, M. W. (1993) *J. Biol. Chem. 268*, 5974−5978.
47. Kim, H.-Y., LaVaute, T., Iwai, K., Klausner, R. D., and Rouault, T. A. (1996) *J. Biol. Chem. 271*, 24226−24230.
48. Casey, J. L., Hentze, M. W., Koeller, D. M., Caughman, S. W., Rouault, T. A., Klausner, R. D., and Harford, J. B. (1988) *Science 240*, 924−928.

BI9924765